ACS Sustainable Chemistry & Engineering

Research Article

pubs.acs.org/journal/ascecg

Electrochemical Hydrogen Pump with SPEEK/CrPSSA Semi-Interpenetrating Polymer Network Proton Exchange Membrane for H_2/CO_2 Separation

Xuemei Wu, Gaohong He,* Lu Yu, and Xiangcun Li

State Key Laboratory of Fine Chemicals, Research and Development Center of Membrane Science and Technology, Dalian University of Technology, 2 Linggong Rd., Hi-Tech Zone, Dalian 116024, P.R. China

ABSTRACT: The possibility of using a nonfluorinated proton exchange membrane for H_2/CO_2 separation in an electrochemical hydrogen pump has been evaluated for the purpose of reducing cost. A sulfonated poly(ether ether ketone) (SPEEK)/cross-linked poly(styrene sulfonic acid) (CrPSSA) semi-interpenetrating polymer network membrane exhibits a much higher proton conductivity (0.09 S cm^{-1} at 80 °C) and humidity sensitivity as compared with the pristine SPEEK membrane. Performance of the hydrogen pump with the sIPN membrane is investigated in different CO_2 contents. The limiting currents are around 0.5−0.6 A and decrease with an increase in CO_2 content, which indicates the transition of the dominant resistance from ohmic resistance to mass transport resistance. Energy efficiency of the SPEEK/CrPSSA-based hydrogen pump is around 30%, which is only slightly lower than that of the Nafion-based hydrogen pump (around 40%) reported in the literature. The results presented here suggest that a nonfluorinated membrane-based hydrogen pump could be promising for hydrogen purification.

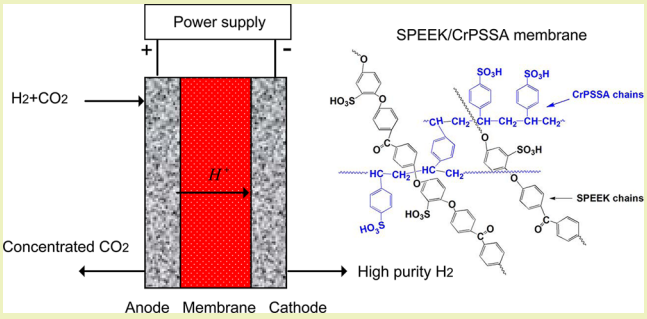

KEYWORDS: *Electrochemical hydrogen pump, Hydrogen purification, Proton exchange membranes, Interpenetrating polymer networks, Sulfonated poly (ether ether ketone)*

INTRODUCTION

H_2/CO_2 separation is an important process to produce hydrogen, which is one of the clean and sustainable energy sources. There are several technologies used in industry, such as amine scrubbing, pressure swing adsorption, cryogenic separation, and membrane separation.[1] Nevertheless, electrochemical hydrogen pump is receiving more attention because it produces pure hydrogen (99.7% and more) in an environmentally friendly way.[2] With an external potential applied, hydrogen in the mixture is oxidized to protons at the anode, which are transported across the polymer electrolyte membrane and reduced to hydrogen again at the cathode. Many investigations reported hydrogen recovery from hydrogen-rich fuels (H_2/N_2, $H_2/CO_2/CO$, H_2/CH_2) or hydrogen of low concentration.[3−6] Other advantages for hydrogen pump separation are related to the ability of compressing hydrogen up to 50 bar at the cathode and the capture of concentrated CO_2 effluent at the anode without further regeneration.[7,8]

The significant challenges for hydrogen pump separation are CO poisoning and cost. Merely trace CO may cause serious poisoning of the Pt catalyst. Periodic pulsing of the applied potential and the polybenzimidazole high temperature membrane (~160 °C) were proposed to improve tolerance to CO.[9,10] The total cost of the hydrogen pump is mainly the cost of the catalyst (Pt) and proton exchange membrane (Nafion). In our previous work, we chose the more abundant metal Pd as the catalyst for reformate separation and investigated the electrochemical activity.[11] However, to our knowledge, there are few investigations focusing on the alternative membranes to Nafion to reduce the cost of hydrogen pumps.

Nonflourinated proton exchange membranes (PEMs) are cost-effective membranes. During fuel cells operations, many nonfluorinated PEMs exhibit high water uptake and comparable electrochemical properties as compared with Nafion.[12−14] Being different from fuel cells, there is no water produced in the operation of the hydrogen pump. The hydration of the membranes completely depends on the external humidification. Therefore, it is necessary to investigate the performance of nonfluorinated PEMs in hydrogen pump applications.

In the present study, sulfonated poly(ether ether ketone) (SPEEK) is used as the polymer matrix. Highly acidic cross-linked poly(styrene sulfonic acid) (CrPSSA) is incorporated into SPEEK to improve proton conductivity by the method of semi-interpenetrating polymer works (SPEEK/CrPSSA

Special Issue: Sustainable Chemical Product and Process Engineering

Received: September 1, 2013
Revised: November 6, 2013
Published: November 10, 2013

sIPN).[15] The obtained sIPN membranes exhibit good compatibility because of the entanglement between polymer chains.[16−19] A catalyst-coated sIPN membrane is prepared to assemble the hydrogen pump. The steady-state current−potential relationship and potential losses, as well as energy efficiency, are investigated in detail.

EXPERIMENTAL SECTION

Materials. PEEK resin is VESTAKEEVR 4000G. Sodium 4-styrenesulfonate (NaSS), divinyl benzene (DVB), benzoyl peroxide (BPO), N-methyl-2-pyrrolidone (NMP), and other chemicals were analytical grade and used as received. Twenty wt% Pt/C catalyst was purchased from Premetek Co. Nafion in methanol is from Ion Power. The gas diffusion layer (GDL) is from SGL Tech. German, GDL 35BC.

Preparation of SPEEK/CrPSSA sIPN membrane. Preparation of the SPEEK/CrPSSA sIPN membrane is according to a procedure in our previous work.[15,20] PEEK is sulfonated homogeneously in 95% concentrated sulfuric acid at 60 °C for 50 min. Semi-interpenetrating polymer networks are prepared by in situ polymerization of NaSS in the solution of SPEEK in a 95 °C oven for 24 h, using BPO as the initiator and DVB as the cross-linker. The weight ratio of NaSS to SPPESK is 1:2. The resulting solution was cast on a glass plate and kept in 40 °C oven for 3 days to evaporate the solvent. The membrane is further protonated and purified by boiling in 0.5 M sulfuric acid/deionized water sequentially for 1 h each. Ion exchange capacities (IECs) of the SPEEK and sIPN membranes are 1.80 and 2.39 mmol g^{-1}, respectively. Thicknesses of the dry membranes are around 100 μm. As shown in Figure 1, the cross-linked CrPSSA chains

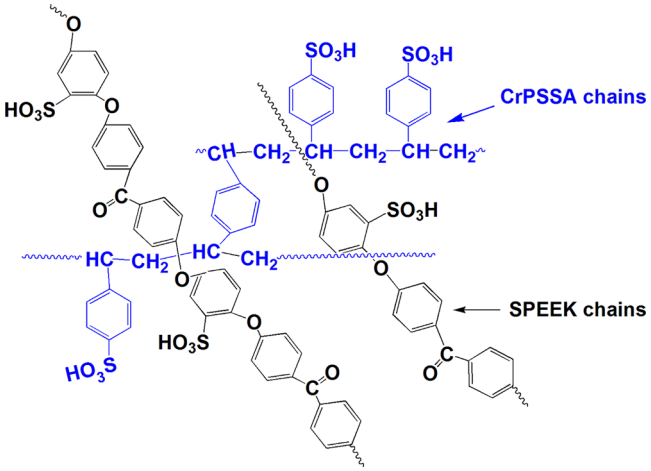

Figure 1. Structure of the SPEEK/CrPSSA sIPN membrane.

interpenetrate with the linear SPEEK chains. In our previous studies, one single glass transition temperature (T_g) of the sIPN was measured by differential scanning calorimetric measurement and suggested good miscibility of the CrPSSA and SPEEK in the sIPN.[15]

Hydrogen Pump Test. The catalyst-coated membrane (CCM) was prepared by air-brushing the catalysts ink (20 wt % Pt/C catalyst suspended in solubilized Nafion in methanol) onto the sIPN membrane. Catalyst loading is about 0.5 mg cm^2. The obtained CCM is sandwiched in two pieces of GDL to prepare the membrane electrode assembly (MEA). The hydrogen pump used in this study is based on the one-dimensional stirred tank reactor (STR) design developed by Benziger and co-workers.[2,21] MEA in the STR had a nominal electrode/electrolyte area of 1.9 cm^2.

The flowchart of the hydrogen pump is similar to that in our previous work and shown in Figure 2.[11] Hydrogen and carbon dioxide are mixed, humidified, and fed into the anode compartment. The electrochemical reactions on the electrodes are shown in Figure 2. By the electrode catalyst, hydrogen can be oxidized to protons at the

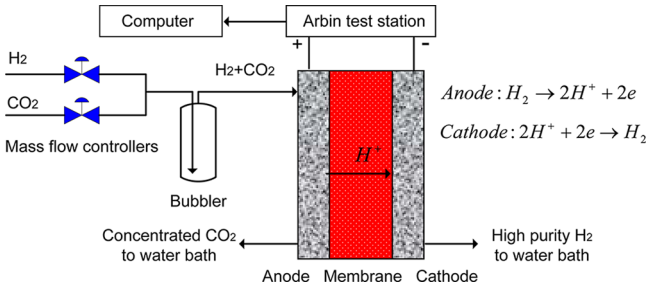

Figure 2. Setup of the electrochemical hydrogen pump for hydrogen purification.

anode and reduced to hydrogen again at the cathode. Carbon dioxide is inert and is concentrated in the anode effluent. The operating temperature of the hydrogen pump is 80 °C. Temperature of the bubbler is 10 °C higher than that of the hydrogen pump in order to get fully humidification of the feed gas. The inlet of the cathode is sealed to keep high partial pressure of hydrogen in the cathode compartment. The flow rate of the dry H_2 and CO_2 mixture is kept as 16 mL min^{-1}, so that flow control dynamics is decoupled from reactor dynamics. CO_2 molar contents in the mixture are similar to that in reformate, e.g., 20% and 25%, respectively.

An Arbin potentiostat/galvanostat data acquisition system is used to provide programmed applied potential ($V_{applied}$) and record the corresponding current (I) and internal resistance (R_{int}). Current−voltage polarization curves are recorded for Tafel analysis, using the current ramp schedule from 0 to 0.1 A at a rate of 5 mA s^{-1}. The steady-state currents are obtained by programming an increase in the applied potential from 0.04 to 0.32 V at an interval of 0.04 V, followed by 0.4, 0.5, and 0.55 V, equilibrated for 0.5 h at each applied potential. The internal resistance of the hydrogen pump is measured by current interruptions in 30 min time intervals. The ohmic resistance, including both the membrane resistance and the ohmic resistance of the ionomer in the catalyst layer, are measured by current interrupt method.

RESULTS AND DISCUSSION

Proton Conductivity of sIPN Membrane. In the sIPN membrane, cross-linked PSSA is incorporated into SPEEK for the purpose of conductivity improving. Figure 3 shows the water uptake and proton conductivity as a function of relative humidity (RH) at 80 °C. Both SPEEK/CrPSSA sIPN and SPEEK membranes exhibit much higher water uptake as compared with that of Nafion (about 34% in water),[14] which is a typical feature of the nonfluorinated PEMs. As compared with

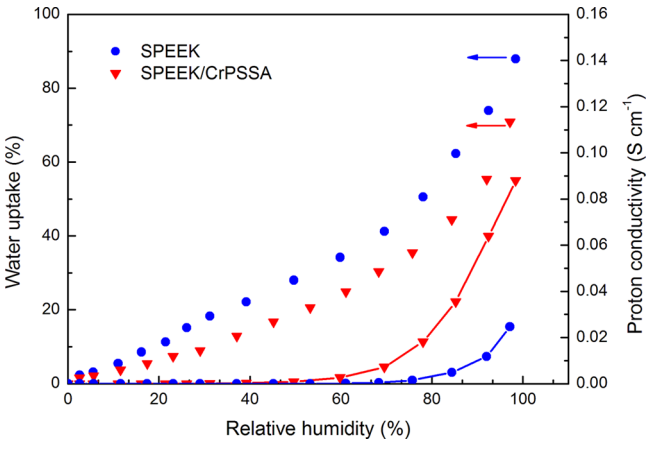

Figure 3. Proton conductivity and water uptake as a function of RH at 80 °C.

dx.doi.org/10.1021/sc400329s | ACS Sustainable Chem. Eng. 2014, 2, 75−79

the SPEEK membrane, the sIPN membrane exhibits lower water uptake but higher proton conductivity. The possible reason is discussed in our previous work[15] and is briefly summarized as follows. The lower water uptake in the sIPN membrane is due to the entanglements between SPEEK and cross-linked PSSA polymer chains. The higher proton conductivity in the sIPN membrane is related to the well connection of the proton pathways. Because the benzyl sulfonic acid side chain of PSSA has very high density and close packing (see Figure 1 for the structure of the sIPN), it is likely to form an elongated ionic cluster in the sIPN membrane and make a continuous pathway for proton transport. As a result, proton conductivity of the sIPN membrane is more sensitive to RH than that of the SPEEK membrane and begins to increase exponentially from RH about 50%. At high RH, proton conductivity of the sIPN membrane is about 3 times that of the SPEEK membrane and is comparable to that of Nafion (0.08–0.1 S cm^{-1}).[13,22]

Steady-State Current of the Hydrogen Pump. A programmed schedule of the applied potential is used to drive the electrochemical reactions on the electrodes. The obtained current and internal resistance are recorded and are shown in Figure 4. The 0.5 h hold at each applied potential

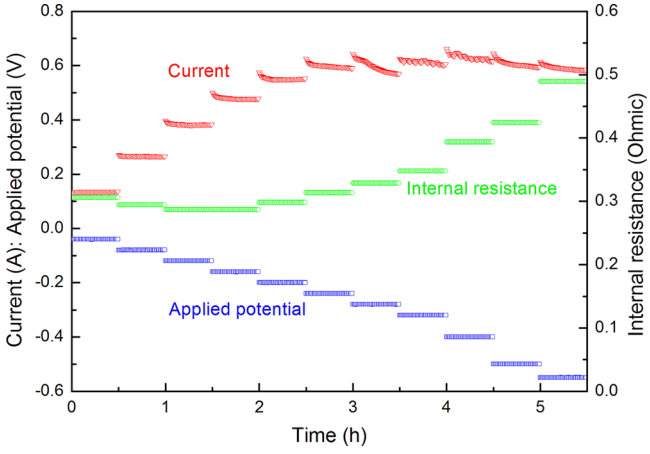

Figure 4. Applied potential, current, and internal resistance measured as a function of testing time.

guarantees the achievement of the steady state. Moles of hydrogen pumped to the cathode can be calculated by the current produced, according to Faraday's law. Figure 4 shows that with an increase in the applied potential, the current increases fast until the limiting current is reached. At the same time, internal resistance gradually increases from 0.3 to 0.5 Ω with an increase in the applied potential, indicating the gradually dehydration of the sIPN membrane at high current. The internal resistance is greater than that of the Nafion-based MEA (0.1–0.2 Ω),[2,15,23] although the sIPN membrane shows comparable proton conductivity to that of Nafion at high RH. This might be related to the incompatible nature between the SPEEK/CrPSSA membrane and the Nafion adhesive in the catalyst ink. It causes higher interfacial resistance. MEA based on SPEEK/PSSA binder instead of Nafion is developing in our group to reduce the interfacial resistance.

In the experiment, flow rate of the H_2/CO_2 at the anode is fixed to 16 mL min^{-1} to investigate the influence of CO_2 content on the current. Figure 5 shows the average current of each 0.5 h hold as a function of the applied potential. With an

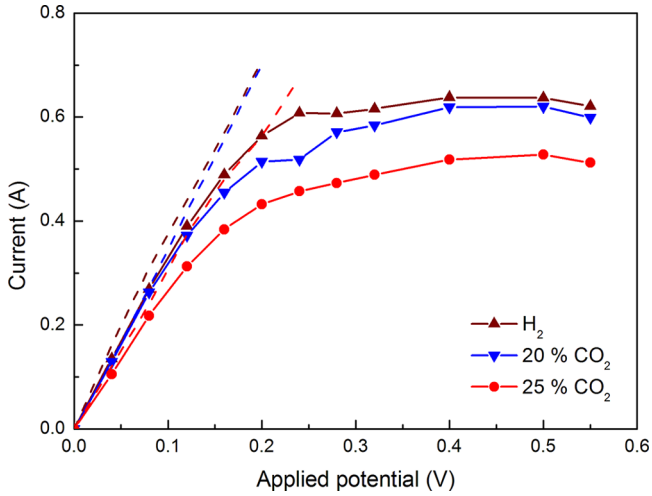

Figure 5. Current as a function of applied potential with different CO_2 content at 80 °C, 16 mL inlet.

increase in the applied potential, the current increases fast until the limiting current is reached. The limiting currents are much lower than the stoichiometric values (1.2 A) and decrease with an increase in CO_2 content from 0.6 A (pure hydrogen) to 0.5 A (25% CO_2). The current is higher than that reported in some literature, for example, about 0.3 A for 20% CO_2 with a 37.5 mL min^{-1} flow rate at the anode.[9] The dashed lines are ohmic currents calculated according to the applied potential divided by the corresponding internal resistance. It is shown that the measured current and ohmic current are comparable at low applied potential, which indicates that ohmic loss is the major resistance in the hydrogen pump. With an increase in applied potential, the difference between the measured current and ohmic current increases gradually, which indicates that other losses such as mass transport resistance contribute more to the difference.

Dominant Resistance Analysis. It is essential to analyze the contributions of different potential losses to the total applied potential in order to determine the dominant resistance and further improve the performance of the hydrogen pump. The applied potential of the hydrogen pump is consumed by the equilibrium loss, activation loss, ohmic loss, and mass transport loss. Equilibrium loss V_{Nerst} of the hydrogen pump is given by Nernst equation (eq 1). V_0 is zero for the hydrogen pump at standard state. The partial pressures of hydrogen at both anode p_{H_2} and cathode $p_{H_{2,cathode}}$ can be calculated according to Benziger's model for the stir tank reactor.[2] Activation loss $V_{activation}$ is related to the sluggish of electrochemical reaction. It can be estimated from eq 2 by assuming that the Tafel slope obtained at low current densities can be extrapolated to the high desired current regime. It is shown in Figure 6 that Tafel slope, b, increases with an increase in CO_2 content, but the values are quite small. The results indicate a slight poisoning of the Pt catalyst by CO_2. Mass transport loss can then be calculated by subtracting the other potential losses from the applied potential, as given by eq 4.

$$V_{Nerst} = V_0 + \frac{RT}{2F}\ln\frac{p_{H_2,cathode}}{p_{H_2,anode}} \quad (1)$$

dx.doi.org/10.1021/sc400329s | ACS Sustainable Chem. Eng. 2014, 2, 75–79

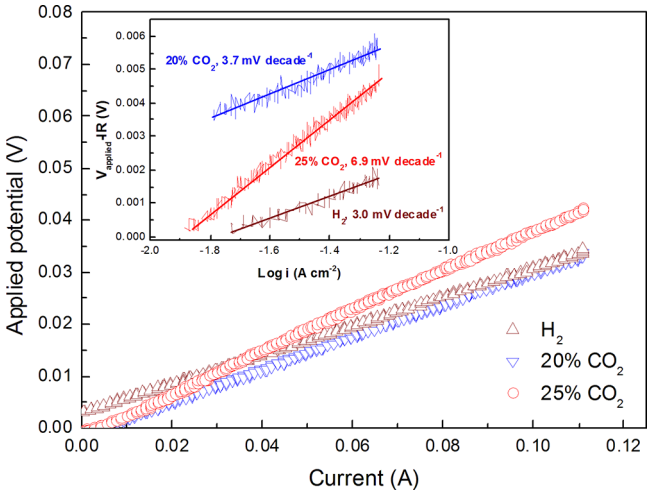

Figure 6. Polarization curve and IR-corrected Tafel plots.

$$V_{\text{activation}} = V_{\text{anode}} + V_{\text{cathode}} = b_{(C/H)}\lg\left(\frac{i}{i_{0,(C/H)}}\right) \quad (2)$$

$$V_{\text{ohmic}} = IR_{\text{int}} \quad (3)$$

$$V_{\text{mass transport}} = V_{\text{applied}} - V_{\text{Nerst}} - V_{\text{activation}} - V_{\text{ohmic}} \quad (4)$$

Figure 7 shows the contributions of different potential losses to the applied potential in a hydrogen pump operating with a

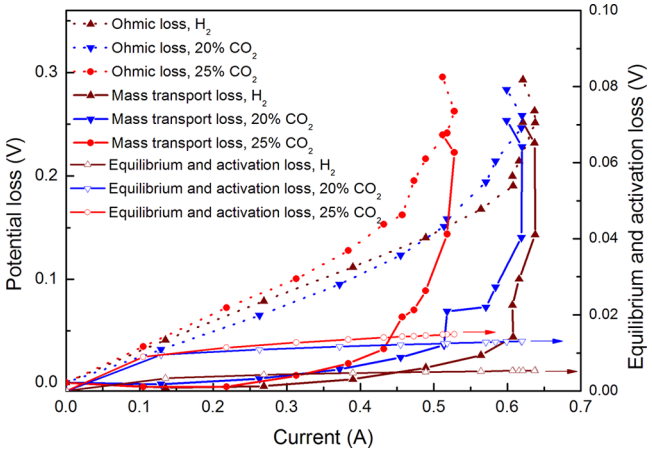

Figure 7. Potential losses in hydrogen pump operating with Pt/C-SPEEK/CrPSSA-Pt/C MEA.

SPEEK/CrPSSA sIPN membrane. It is shown that the sum of the equilibrium and activation losses are at least 1 order of magnitude smaller than that of the ohmic and mass transport losses, and thus they can be ignored. The dominant potential loss at low current is ohmic loss. It increases linearly with an increase in current. The rapid increase in ohmic loss at high current is related to the redistribution of water in the membrane due to high electro-osmotic drag,[24] while mass transport loss increases exponentially with an increase in current and becomes dominant at high current. The crossover point indicates the transition of the dominant potential loss from ohmic loss to mass transport loss and coincides with the limiting current appearing at high current regime as shown in Figure 5. With an increase in CO_2 content, the transition current shifted to lower value, which indicates the higher mass transport resistance caused by CO_2. As CO_2 in the feed gas cannot be pumped across the membrane, it accumulates in the porous media (especially in the catalyst layer) and blocks hydrogen diffusion and convection, as we discussed in our previous work.[11] Concentration polarization of the anode feed can be ignored because with the stir tank reactor design of the hydrogen pump, the anode behaves as a perfectly mixed unit;[2,21] therefore, the composition in the anode flow channel is uniform and the same as the effluent.

The results indicate that there are two dominant resistances: first, ohmic resistance, and then mass transport resistance in the hydrogen pump. Even in the mass transport loss regime, ohmic loss still plays an important role in the limiting current of the hydrogen pump. With the improvement in the proton conductivity of the sIPN membrane, the limiting current can be improved. The relationship between sIPN structure and the limiting current is interesting and needs to be investigated further.

Efficiency of the Hydrogen Pump. Hydrogen recovery and energy efficiency of the hydrogen pump with the sIPN membrane are calculated according to eqs 5 and 6[2] and plotted in Figure 8. Hydrogen recovery is the fraction of hydrogen

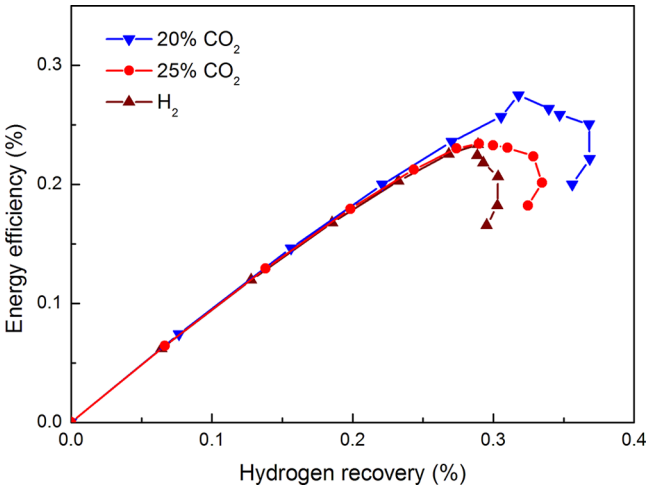

Figure 8. Energy efficiency as a function of hydrogen recovery.

released at the cathode in the anode feed (q_{n,feed,H_2}). Energy efficiency is defined as the net energy recovered (energy contained in the product hydrogen minus the energy consumed by the potential applied) divided by the total energy contained in the hydrogen feed in the anode. $\Delta H_{\text{combusion}}$ is the heat of combustion of hydrogen. It is shown in Figure 8 that all data points fall on the same line and are independent of CO_2 content when energy efficiency are less than 20%. This indicates that energy efficiency in this regime is dominated by ohmic resistance. The maximum energy efficiency suggests the transition of dominant resistance. After that, the mass transport limiting current leads to a decrease in energy efficiency. The maximum energy efficiency is also related to the total hydrogen feed in the anode. The lowest energy efficiency is observed for pure hydrogen, which is due to the highest total energy contained in the anode feed, despite the highest hydrogen concentration of pure hydrogen, while the 25% CO_2 feed has the highest mass transport resistance, resulting in the lower energy efficiency as compared with the 20% CO_2 feed.

dx.doi.org/10.1021/sc400329s | ACS Sustainable Chem. Eng. 2014, 2, 75−79

$$\text{Hydrogen recovery} = \frac{I}{2Fq_{n,\text{feed},H_2}} \quad (5)$$

$$\text{Energy efficiency} = = \frac{\frac{I}{2F}\Delta H_{\text{combustion}} - IV_{\text{applied}}}{q_{n,\text{feed},H_2}\Delta H_{\text{combustion}}} \quad (6)$$

As shown in Figure 8, operating with a SPEEK/CrPSSA sIPN membrane leads to a maximum energy efficiency of about 30%, which is slightly lower than the reported 40% with the Nafion membrane in the literature.[2] Taking the low cost into account, the SPEEK/CrPSSA membrane could be promising for hydrogen pump purification. Because energy efficiency is controlled by resistances both in the membranes and in the gas diffusion media, progress in these areas would helpful to improve performance of hydrogen pumps.

CONCLUSIONS

Hydrogen purification from a CO_2/H_2 mixture is performed on an electrochemical hydrogen pump with a SPEEK/CrPSSA semi-interpenetrating polymer network membrane. Proton conductivity of the sIPN membrane is about 3 times that of the pristine SPEEK membrane due of the interpenetration of the highly acidic cross-linked PSSA into the SPEEK backbone. With an increase in the applied potential, current increases linearly until the limiting current is reached. Energy efficiency of the hydrogen pump reaches a maximum with an increase in hydrogen recovery. The results indicate that there are two dominant resistances in the hydrogen pump, e.g., ohmic resistance and mass transport resistance. The limiting currents decrease with an increase in CO_2 content, from 0.6 A (pure hydrogen) to 0.5 A (25% CO_2), which suggests a greater mass transport resistance caused by CO_2 accumulation in the porous media. Energy efficiency of the SPEEK/CrPSSA-based hydrogen pump is around 30%, which is only slightly lower than that of the Nafion-based hydrogen pump reported in the literature. Because the sIPN nonfluorinated membrane is much cheaper than Nafion, it could be promising for hydrogen pump purification.

AUTHOR INFORMATION

Corresponding Author

*Tel: +86 411 84986291. E-mail: hgaohong@dlut.edu.cn.

Notes

The authors declare no competing financial interest.

ACKNOWLEDGMENTS

The authors thank the Program for National Science Fund for Distinguished Young Scholars of China (Grant 21125628) and NSFC (Grant 20976027 and 21176044) for financial support of this work.

REFERENCES

(1) Holladay, J. D.; Hu, J.; King, D. L.; Wang, Y. An overview of hydrogen production technologies. *Catal. Today* **2009**, *139*, 244−260.
(2) Abdulla, A.; Laney, K.; Padilla, M.; Sundaresan, S.; Benziger, J. Efficiency of hydrogen recovery from reformate with a polymer electrolyte hydrogen pump. *AIChE J.* **2011**, *57*, 1767−1779.
(3) Ibeh, B.; Gardner, C.; Ternan, M. Separation of hydrogen from a hydrogen/methane mixture using a PEM fuel cell. *Int. J. Hydrogen Energy* **2007**, *32*, 908−914.
(4) Lee, H. K.; Choi, H. Y.; Choi, K. H.; Park, J. H.; Lee, T. H. Hydrogen separation using electrochemical method. *J. Power Sources* **2004**, *132*, 92−98.
(5) Onda, K.; Araki, T.; Ichihara, K.; Nagahama, M. Treatment of low concentration hydrogen by electrochemical pump or proton exchange membrane fuel cell. *J. Power Sources* **2009**, *188*, 1−7.
(6) Barbir, F.; Gorgun, H. Electrochemical hydrogen pump for recirculation of hydrogen in a fuel cell stack. *J. Appl. Electrochem.* **2007**, *37*, 359−365.
(7) Grigoriev, S. A.; Shtatniy, I. G.; Millet, P.; Porembsky, V. I.; Fateev, V. N. Description and characterization of an electrochemical hydrogen compressor/concentrator based on solid polymer electrolyte technology. *Int. J. Hydrogen Energy* **2011**, *36*, 4148−4155.
(8) Casati, C.; Longhi, P.; Zanderighi, L.; Bianchi, F. Some fundamental aspects in electrochemical hydrogen purification/compression. *J. Power Sources* **2008**, *180*, 103−113.
(9) Gardner, C. L.; Ternan, M. Electrochemical separation of hydrogen from reformate using PEM fuel cell technology. *J. Power Sources* **2007**, *171*, 835−841.
(10) Perry, K. A.; Eisman, G. A.; Benicewicz, B. C. Electrochemical hydrogen pumping using a high-temperature polybenzimidazole (PBI) membrane. *J. Power Sources* **2008**, *177*, 478−484.
(11) Wu, X.; Benziger, J.; He, G. Comparison of Pt and Pd catalysts for hydrogen pump separation from reformate. *J. Power Sources* **2012**, *218*, 424−434.
(12) Maier, G.; Haack, J. M. Sulfonated aromatic polymers for fuel cell membranes. *Adv. Polym. Sci.* **2008**, *216*, 1−62.
(13) Du, L.; Yan, X.; He, G.; Wu, X.; Hu, Z.; Wang, Y. SPEEK proton exchange membranes modified with silica sulfuric acid nanoparticles. *Int. J. Hydrogen Energy* **2012**, *37*, 1853−1861.
(14) Xing, D.; He, G.; Hou, Z.; Ming, P.; Song, S. Preparation and characterization of a modified montmorillonite/sulfonated polyphenylether sulfone/PTFE composite membrane. *Int. J. Hydrogen Energy* **2011**, *36*, 2177−2183.
(15) Wu, X.; He, G.; Li, X.; Nie, F.; Yan, X.; Yu, L.; Benziger, J. Improving proton conductivity of sulfonated poly (ether ether ketone) proton exchange membranes at low humidity by semi-interpenetrating polymer networks preparation. *J. Power Sources* **2014**, *246*, 482−490.
(16) Wu, X.; He, G.; Gu, S.; Hu, Z.; Yao, P. Novel interpenetrating polymer network sulfonated poly(phtalazione ether sulfone ketone)/polyacrilic acid proton exchange membranes for fuel cell. *J. Membr. Sci.* **2007**, *295*, 80−87.
(17) Wu, X.; He, G.; Gu, S.; Hu, Z.; Yan, X. The state of water in the series of sulfonated poly (phthalazinone ether sulfone ketone) (SPPESK) proton exchange membranes. *Chem. Eng. J.* **2010**, *156*, 578−581.
(18) Chikh, L.; Delhorbe, V.; Fichet, O. (Semi-) Interpenetrating polymer networks as fuel cell membranes. *J. Membr. Sci.* **2011**, *368*, 1−17.
(19) Lipatov, Y. S.; Alekseeva, T. T. Phase-separated interpenetrating polymer networks. *Adv. Polym. Sci.* **2007**, *208*, 1−227.
(20) Wu, X.; Wang, X.; He, G.; Benziger, J. Differences in water sorption and proton conductivity between Nafion and SPEEK. *J. Polym. Sci., Part B: Polym. Phys.* **2011**, *49*, 1437−1445.
(21) Benziger, J.; Chia, E.; Karnas, E.; Moxley, J.; Teuscher, C.; Kevrekidis, I. G. The stirred tank reactor polymer electrolyte membrane fuel cell. *AIChE J.* **2004**, *50*, 1889−1900.
(22) Kumar, G. G.; Kim, A. R.; Nahm, K. S.; Elizabeth, R. Nafion membranes modified with silica sulfuric acid for the elevated temperature and lower humidity operation of PEMFC. *Int. J. Hydrogen Energy* **2009**, *34*, 9788−9794.
(23) Sedlak, J. M.; Austin, J. F.; Laconti, A. B. Hydrogen recovery and purification using the solid polymer electrolyte electrolysis cell. *Int. J. Hydrogen Energy* **1981**, *6*, 45−51.
(24) Cheah, M. J.; Kevrekidis, I. G.; Benziger, J. *J. Phys. Chem. B* **2011**, *115*, 10239−10250.